White light Bessel-like beams generated by miniature all-fiber device

X. Zhu,[1,*] A. Schülzgen,[2] H. Wei,[1] K. Kieu,[1] and N. Peyghambarian[1]

[1]*College of Optical Sciences, University of Arizona, 1630 East University Boulevard, Tucson, Arizona 85721, USA*
[2]*College of Optics and Photonics, CREOL, University of Central Florida, 4000 Central Florida Boulevard, Orlando, Florida 32816 USA*
**xszhu@email.arizona.edu*

Abstract: Micron-sized white light propagation invariant beams generated by a simple and compact fiber device are presented. The all-fiber device is fabricated by splicing a short piece of large-core multimode fiber onto a small-core single mode white light delivery fiber. Because this fiber device offers an inherent spatial coherence, nondiffracting white light beams can be created with a temporally incoherent broadband light source (a halogen bulb) and, most importantly, the surrounding fringes don't fade as the bandwidth of the light source increases because the underlying physics of this fiber device is different from that of the axicon. White light Bessel-like beams have been generated from multimode fibers with core diameters of 50 μm, 105 μm, and 200 μm. The distance of nondiffracting propagation of the white light Bessel beam increases with increasing core size of the multimode fiber. Propagation characteristics of red, green, and blue individual beams are also presented.

OCIS codes: (140.3330) Laser beam shaping; (060.2310) Fiber optics; (230.2285) Fiber devices and optical amplifiers; (260.1960) Diffraction theory.

References and links

1. V. Garcés-Chávez, D. McGloin, H. Melville, W. Sibbett, and K. Dholakia, "Simultaneous micromanipulation in multiple planes using a self-reconstructing light beam," Nature **419**(6903), 145–147 (2002).
2. V. Karásek, T. Cizmár, O. Brzobohatý, P. Zemánek, V. Garcés-Chávez, and K. Dholakia, "Long-range one-dimensional longitudinal optical binding," Phys. Rev. Lett. **101**(14), 143601 (2008).
3. T. Wulle and S. Herminghaus, "Nonlinear optics of Bessel beams," Phys. Rev. Lett. **70**(10), 1401–1404 (1993).
4. K. S. Lee and J. P. Rolland, "Bessel beam spectral-domain high-resolution optical coherence tomography with micro-optic axicon providing extended focusing range," Opt. Lett. **33**(15), 1696–1698 (2008).
5. Y. Matsuoka, Y. Kizuka, and T. Inoue, "The characteristics of laser micro drilling using a Bessel beam," Appl. Phys., A Mater. Sci. Process. **84**(4), 423–430 (2006).
6. M. Fortin, M. Piché, and E. F. Borra, "Optical tests with Bessel beam interferometry," Opt. Express **12**(24), 5887–5895 (2004).
7. M. Erdélyi, Z. L. Horvath, G. Szabo, Zs. Bor, F. K. Tittel, J. R. Cavallaro, and M. C. Smayling, "Generation of diffraction-free beams for application in optical microlithography," J. Vac. Sci. Technol. B **15**(2), 287–292 (1997).
8. J. Durnin, "Exact solutions for nondiffracting beams. I. The scalar theory," J. Opt. Soc. Am. A **4**(4), 651–654 (1987).
9. J. Durnin, J. J. Miceli, Jr., and J. H. Eberly, "Diffraction-free beams," Phys. Rev. Lett. **58**(15), 1499–1501 (1987).
10. G. Indebetouw, "Nondiffracting optical fields: some remarks on their analysis and synthesis," J. Opt. Soc. Am. A **6**(1), 150–152 (1989).
11. J. A. Davis, E. Carcole, and D. M. Cottrell, "Nondiffracting interference patterns generated with programmable spatial light modulators," Appl. Opt. **35**(4), 599–602 (1996).
12. A. Vasara, J. Turunen, and A. T. Friberg, "Realization of general nondiffracting beams with computer-generated holograms," J. Opt. Soc. Am. A **6**(11), 1748–1754 (1989).
13. S. K. Eah, W. Jhe, and Y. Arakawa, "Nearly diffraction-limited focusing of a fiber axicon microlens," Rev. Sci. Instrum. **74**(11), 4969–4971 (2003).
14. S. Cabrini, C. Liberale, D. Cojoc, A. Carpentiero, M. Prasciolou, S. Mora, V. Degiorgio, F. De Angelis, and E. Di Fabrizio, "Axicon lens on optical fiber forming optical tweezers, made by focused ion beam milling," Microelectron. Eng. **83**(4-9), 804–807 (2006).

#143457 - $15.00 USD Received 2 Mar 2011; revised 27 Apr 2011; accepted 15 May 2011; published 26 May 2011

15. T. Grosjean, S. S. Saleh, M. A. Suarez, I. A. Ibrahim, V. Piquerey, D. Charraut, and P. Sandoz, "Fiber microaxicons fabricated by a polishing technique for the generation of Bessel-like beams," Appl. Opt. **46**(33), 8061–8067 (2007).
16. V. S. Ilchenko, M. Mohageg, A. A. Savchenkov, A. B. Matsko, and L. Maleki, "Efficient generation of truncated Bessel beams using cylindrical waveguides," Opt. Express **15**(9), 5866–5871 (2007).
17. J. K. Kim, J. Kim, Y. Jung, W. Ha, Y. S. Jeong, S. Lee, A. Tünnermann, and K. Oh, "Compact all-fiber Bessel beam generator based on hollow optical fiber combined with a hybrid polymer fiber lens," Opt. Lett. **34**(19), 2973–2975 (2009).
18. M. Brunel and S. Coetmellec, "Generation of nondiffracting beams through an opaque disk," J. Opt. Soc. Am. A **24**(12), 3753–3761 (2007).
19. E. McLeod, A. B. Hopkins, and C. B. Arnold, "Multiscale Bessel beams generated by a tunable acoustic gradient index of refraction lens," Opt. Lett. **31**(21), 3155–3157 (2006).
20. X. Zhu, A. Schülzgen, L. Li, and N. Peyghambarian, "Generation of controllable nondiffracting beams using multimode optical fibers," Appl. Phys. Lett. **94**(20), 201102 (2009).
21. S. Ramachandran and S. Ghalmi, "'Diffraction-free,' self-healing bessel beams from fibers," in *Conference on Lasers and Electro-Optics/Quantum Electronics and Laser Science Conference and Photonic Applications Systems Technologies*, OSA Technical Digest (CD) (Optical Society of America, 2008), paper CPDB5.
22. L. Basano and P. Ottonello, "Demonstration experiments on nondiffracting beams generated by thermal light," Am. J. Phys. **73**(9), 826–830 (2005).
23. P. Fischer, C. T. A. Brown, J. E. Morris, C. López-Mariscal, E. M. Wright, W. Sibbett, and K. Dholakia, "White light propagation invariant beams," Opt. Express **13**(17), 6657–6666 (2005).
24. P. Fischer, H. Little, R. L. Smith, C. Lopez-Mariscal, C. T. A. Brown, W. Sibbett, and K. Dholakia, "Wavelength dependent propagation and reconstruction of white light Bessel beams," J. Opt. A, Pure Appl. Opt. **8**(5), 477–482 (2006).
25. J. Leach, G. M. Gibson, M. J. Padgett, E. Esposito, G. McConnell, A. J. Wright, and J. M. Girkin, "Generation of achromatic Bessel beams using a compensated spatial light modulator," Opt. Express **14**(12), 5581–5587 (2006).
26. T. Cižmár, V. Kollárová, X. Tsampoula, F. Gunn-Moore, W. Sibbett, Z. Bouchal, and K. Dholakia, "Generation of multiple Bessel beams for a biophotonics workstation," Opt. Express **16**(18), 14024–14035 (2008).
27. X. Zhu, A. Schülzgen, H. Li, L. Li, L. Han, J. V. Moloney, and N. Peyghambarian, "Detailed investigation of self-imaging in large-core multimode optical fibers for application in fiber lasers and amplifiers," Opt. Express **16**(21), 16632–16645 (2008).
28. X. Zhu, A. Schülzgen, H. Li, H. Wei, J. V. Moloney, and N. Peyghambarian, "Coherent beam transformations using multimode waveguides," Opt. Express **18**(7), 7506–7520 (2010).
29. X. Zhu, A. Schülzgen, H. Li, L. Li, V. L. Temyanko, J. V. Moloney, and N. Peyghambarian, "High power fiber lasers and amplifiers based on multimode interference," IEEE J. Sel. Top. Quantum Electron. **15**(1), 71–78 (2009).

1. Introduction

Due to their unique properties of nondiffracting propagation and self-reconstruction, Bessel beam has found applications in optical trapping and manipulation [1], optical binding [2], nonlinear optics [3], optical coherent tomography [4], microfabrication [5], interferometry [6], and lithography [7] since it was first proposed and demonstrated by Durnin [8,9] in 1987. Motivated by considerable practical and potential applications, people have proposed a variety of methods to generate Bessel beam. Most of these techniques are based on the physics that a Bessel beam results from the interference of plane waves propagating on a conic surface and usually use bulk and free-space optical components such as an annular aperture located at the focal plane of a lens [9], axicon [10], spatial light modulator [11], and computer-generated hologram [12]. The common concept has also been applied to fabricate a compact fiber device that is able to generate micro-sized Bessel beam. Microaxicons [13–15] and whispering gallery mode resonators [16] fabricated on the fiber end have been reported. A compact structure in a serial concatenation of hollow optical fiber, coreless silica fiber, and a polymer lens has also been demonstrated recently [17].

In recent years, several techniques differing from the common concept, such as using an opaque disk [18] or a tunable gradient index of refraction lens [19], have been proposed. Based on the fact that the zeroth-order radial modes (LP_{0n}) of a multimode (MM) optical fiber are mathematically represented by Bessel functions and the high-order LP_{0n} modes are actually truncated Bessel beams [20], two new techniques of generating Bessel beam from optical fibers have been demonstrated [20,21]. When a long-period fiber Bragg grating (FBG) is inscribed into the core of an optical fiber, Bessel beam can be generated from the optical fiber due to the mode coupling between the fundamental core mode and the LP_{0n} cladding modes induced by the long-period FBG [21]. Utilizing the mode coupling from LP_{01} mode to

#143457 - $15.00 USD Received 2 Mar 2011; revised 27 Apr 2011; accepted 15 May 2011; published 26 May 2011

high-order LP_{0n} modes at the interface between a single-mode fiber and a MM fiber, we have demonstrated an extremely simple and low-cost method to generate nondiffracting beams from optical fibers [20]. Compared to the fiber device using a long-period FBG, which is highly wavelength dependent, our device can be applied in a very broad spectral range. Moreover, our device can be used to generate white light Bessel-like beam.

White light Bessel beam may find applications in optical coherence tomography with large depth range resolution, high resolution incoherent interferometry, multi-functional optical trapping, sorting, and manipulation, single molecular fluorescence, and multi-molecular binding. White light Bessel beam generated by the techniques based on the common concept (using axicon or spatial light modulator) has been investigated by several groups [22–25]. In this paper, we demonstrate that white light Bessel-like beam can be generated from our simple fiber device, which is fabricated by just splicing a short piece of multimode fiber onto a single-mode white light delivery fiber. White light propagation invariant beams generated by using multimode fibers with different core diameters and lengths are presented and investigated. Our experimental results confirm that this fiber device may enable multifunctional biophotonics platform [26].

2. Experimental setup and theory

The fiber device is fabricated by splicing a short piece of multimode fiber onto a single mode white light delivery fiber. The white light delivery fiber is Nufern 460-HP fiber, which has a mode field diameter of about 3.5 μm and a numerical aperture (NA) of 0.13. Multimode fibers with diameters of 50 μm, 105 μm, and 200 μm (Thorlabs, AFS50/125Y, AFS105/125Y, and AFS200/220Y) are used in the experiment for the purpose to investigate the dependence of the nondiffracting propagation on the core size of the multimode fiber. All the multimode fibers have a NA of 0.22. It has been realized that spatial coherence is a key criterion for white light Bessel beam propagation [22–24]. Our fiber device offers an inherent highly spatial coherence and consequently nondiffracting white light beam can be achieved with temporally incoherent broadband light source. A fiber-coupled white light source using halogen bulb (Yokogawa AQ4305) is used as the signal source. The signal delivery fiber Nufern 460-HP is connected to the white light source and the spectrum of the white light propagating through a piece of 1.5 meter long signal delivery fiber is measured and shown in Fig. 1. The 460-HP fiber provides a good single transverse mode guiding for the visible light. However, due to the emission spectrum of the halogen bulb and the transmission property of the 460-HP fiber, the power of the blue light is smaller than that of the red light. The experimental setup is shown in Fig. 2. A part of the fiber device including a section of the single mode fiber and the whole segment of the multimode fiber is placed on a v-groove holder. The beam profiles of the Bessel beam at varying distances from the MM fiber facet are

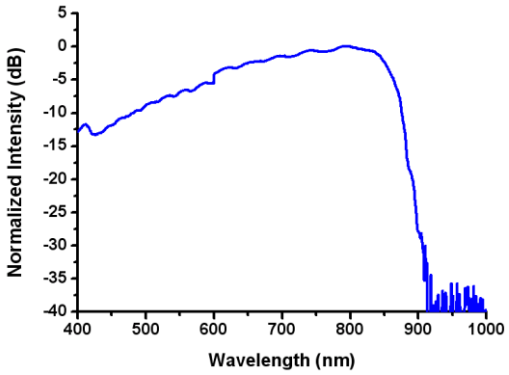

Fig. 1. Spectrum of the white light propagating through a piece of 1.5 meter long single-mode signal delivery fiber.

#143457 - $15.00 USD Received 2 Mar 2011; revised 27 Apr 2011; accepted 15 May 2011; published 26 May 2011

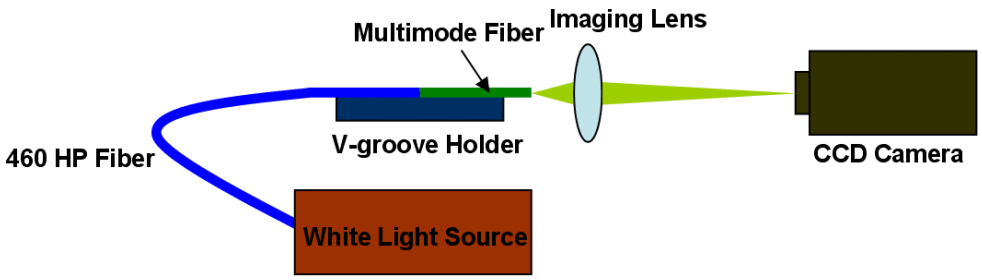

Fig. 2. Experimental setup for characterizing white light Bessel beams generated from multimode fibers. 460-HP fiber (core diameter 3 μm, NA 0.13); Multimode fiber (core diameter 50 μm, 105 μm, and 200 μm, NA 0.22); Imaging lens (focal length 8 mm, NA 0.5).

magnified by an aspheric lens (NA = 0.5, focal length = 8 mm) and recorded by a color CCD camera (Sony, ExWaveHAD). The magnification factor of the imaging system is about 30. The nondiffracting propagation properties of the Bessel beam can be characterized by the evolution of the beam intensity profiles.

Because we have interpreted the physics of non-diffracting beam generation utilizing high-order LP_{0n} mode excitation through the mode coupling from a single mode fiber to a MM fiber in [20], here we briefly describe the theory of the fiber device to generate white light Bessel-like beam. Because the cut-off wavelength of the signal delivery fiber is about 430 nm, single transverse mode of the white light can be delivered to the MM fiber. Due to the mode orthogonality and the on-axis excitation, $LP_{0,n}$ modes (n is the radial index) of the MM fiber are then excited. Because each $LP_{0,n}$ mode propagates along the waveguide independently with its own propagation constant, the field of a wavelength of λ at the output facet of the MM fiber is the superposition of Bessel-like fields

$$E_{\lambda,Out}(r,L)=\sum_{n=1}^{N}C_{\lambda,n}J_0(\kappa_{\lambda,n}r)e^{-i\beta_{\lambda,n}L},\quad r\le R, \tag{1}$$

where N is the number of the strongly excited modes in the MM fiber segment; $C_{\lambda,n}$ is the decomposition coefficient; r is the radial coordinate and smaller than the core radius of the MM fiber R; L is the MM fiber length; the apertured Bessel functions $J_0(\kappa_{\lambda,n}r)$ with different transverse wave vectors, $\kappa_{\lambda,n}=(n_{f\lambda}^2k_\lambda^2-\beta_{\lambda,n}^2)^{1/2}$, represent the fields of the $LP_{0,n}$ modes in the MM fiber core. Here, $k_\lambda=2\pi/\lambda$, $n_{f\lambda}$ is the refractive index of the fiber core at the wavelength of λ, and $\beta_{\lambda,n}$ is the propagation constant of the $LP_{0,n}$ mode of λ, respectively.

The decomposition coefficient $C_{\lambda,n}$ for a single mode input $E_{\lambda,in}$ can be obtained by

$$C_{\lambda,n}=\frac{\iint_S E_{\lambda,in}(r,\varphi)\times J_0^*(k_{\lambda,n}r)ds}{\iint_S\left|J_0(\kappa_{\lambda,n}r)\right|^2ds}. \tag{2}$$

The percentage of the power coupled from the fundamental mode of the single-mode fiber to the $LP_{0,n}$ modes of the MM fibers $|C_{\lambda,n}|^2$ are calculated for the signals of 630 nm, 550nm, and 480 nm, and shown in Fig. 3. Obviously, for all the wavelengths, most power is coupled to high order modes of the MM fiber. It has been demonstrated that nondiffracting propagation is most pronounced when high order $LP_{0,n}$ modes are excited [20]. White light propagation invariant beam can thus be generated from the three large-core MM fibers. As shown in Fig. 3, the larger the MM fiber core, the more high order modes are excited. The longest distance of nondiffracting propagation is expected for the beam coming from the 200 μm core MM fiber.

#143457 - $15.00 USD Received 2 Mar 2011; revised 27 Apr 2011; accepted 15 May 2011; published 26 May 2011

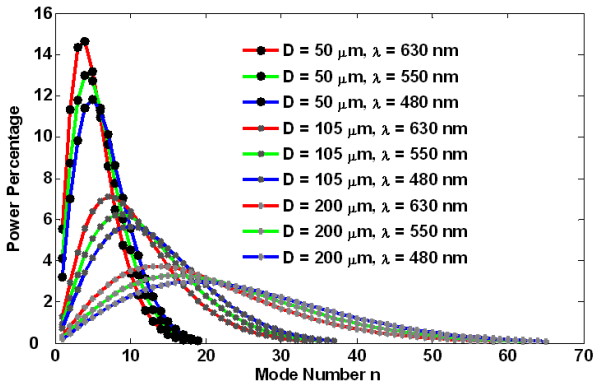

Fig. 3. Percentage of the power coupled from the fundamental mode of the single mode fiber to the $LP_{0,n}$ modes of the multimode fibers with diameters of 50 μm, 105 μm, and 200 μm for the signal wavelengths of 630 nm, 550 nm, and 480 nm.

The field of the beam of the wavelength λ propagating in free space after leaving the fiber can be approximated as

$$E_{\lambda,fs}(r,z)=\sum_{n=1}^{N}C_{\lambda,n}J_0(\kappa_{\lambda,n}r)e^{i(\beta_{nf}z+\beta_n L)} \tag{3}$$

with a propagation constant in free space $\beta_{nf} = (k_\lambda^2-\kappa_{\lambda,n}^2)^{1/2}$. As a consequence of the superposition of multiple Bessel fields, the propagation of the beam of the wavelength λ can be almost diffraction-free and special beam patterns can be generated at certain axial regions [20]. When a broadband light source is used, the intensity profile of the beam can be described as follows,

$$I_{fs}(r,z)=\int_{\lambda}\left|E_{\lambda,fs}(r,z)\right|^2 d\lambda=\int_{\lambda}\left|\sum_{n=1}^{N}C_{\lambda,n}J_0(\kappa_{\lambda,n}r)e^{i(\beta_{nf}z+\beta_n L)}\right|^2 d\lambda. \tag{4}$$

Thus, white light Bessel beam with long propagation invariant distance can be generated through the incoherent addition of the nondiffracting beams of all spectral components.

3. Experimental results

Multimode fibers with core diameters of 50 μm, 105 μm, and 200 μm are used in the experiment. The facet image is recorded by the color CCD camera using the setup shown in Fig. 2. The propagation characteristics of the beam are obtained by recording the intensity profiles of the beam at varying positions along the propagation direction with a step of 5 μm. The far field intensity profile of the beam is recorded by removing the imaging lens and placing the CCD camera at a distance of 2 cm to the MM fiber facet. In order to investigate the propagation characteristics of the individual beam of a spectral component, three band-pass filters with a bandwidth of 10 nm are used in the experiment. Their central wavelengths are 630 nm, 550 nm, and 480 nm, respectively.

When a 2 cm long 50 μm MM fiber is spliced to the 460-HP fiber, the intensity distributions of the white, red, green, and blue light at the MM fiber facet are shown in Figs. 4 (a)-(d). As a result of the incoherent addition of excited LP_{0n} modes of all wavelengths, the intensity profile of the white light has a bright central spot. However, the intensity profiles of the individual beams exhibit different features. The red light profile has a bright central spot. The green and the blue light profiles show a pattern with several rings. The corresponding far-field intensity profiles with a full size of about 8 mm are shown in Figs. 4 (e)-(h). The white light far-field profile exhibits a feature of several color rings and a white central spot. The far-field profiles of the individual beams have different patterns associated with their respective

#143457 - $15.00 USD Received 2 Mar 2011; revised 27 Apr 2011; accepted 15 May 2011; published 26 May 2011

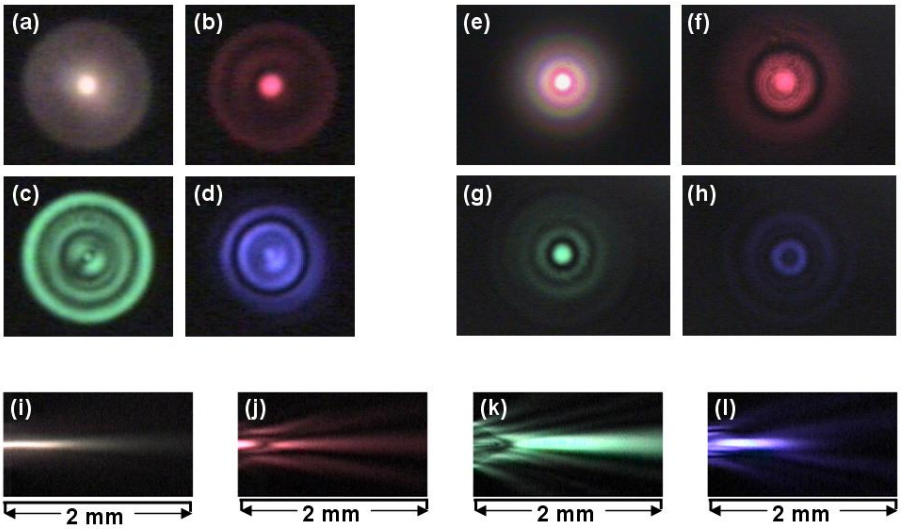

Fig. 4. Facet (a-d) and far-field (e-h) intensity profiles and the propagation characteristics (i-l) of the white Bessel beam and the red (630 nm), green (550 nm), and blue (480 nm) individual beams when a 2 cm long 50 μm multimode fiber is used.

facet fields $E_{\lambda,out}$ (r, L). The beam propagation characteristics of the white, red, green, and blue light are shown in Figs. 4 (i)-(l). Obviously, a white light Bessel-like beam with a nondiffracting propagation of about 1 mm was obtained. As the bandwidth of the light is reduced to 10 nm by use of the band-pass filters, the propagation of the individual beam is different from that of a general zeroth-order Bessel beam. At some certain positions, the intensity profile has not a bright central spot, i.e., the supposition of the excited LP_{0n} modes for individual wavelength is destructive at the beam center.

It is found that, when a piece of 10 cm long 50 μm MM fiber is used, nondiffracting propagation is increased to almost 2 mm as shown in Fig. 5 (i). Moreover, as shown in Figs. 5 (j)-(l), the Bessel-like nondiffracting propagation can be found in the red, green, and blue

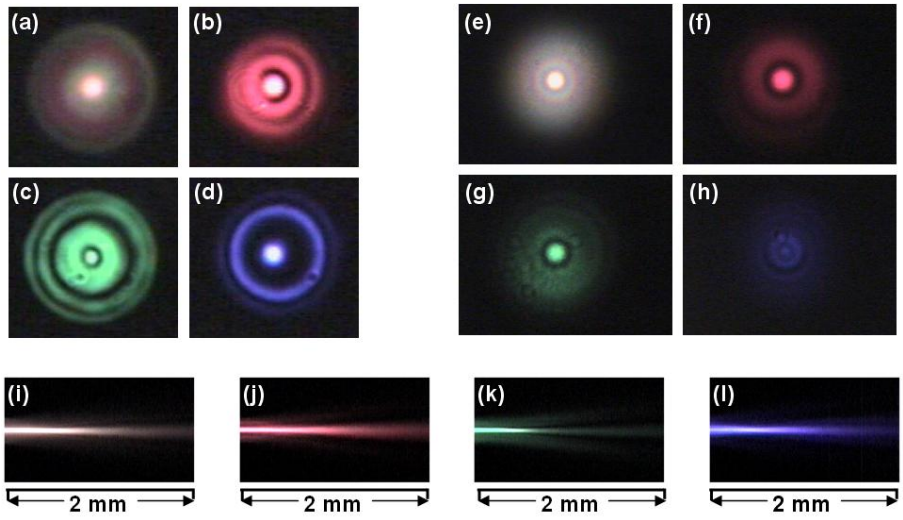

Fig. 5. Facet (a-d) and far-field (e-h) intensity profiles and the propagation characteristics (i-l) of the white Bessel beam and the red (630 nm), green (550 nm), and blue (480 nm) individual beams when a 10 cm long 50 μm multimode fiber is used.

#143457 - $15.00 USD Received 2 Mar 2011; revised 27 Apr 2011; accepted 15 May 2011; published 26 May 2011

individual beams. This is because the wavelength dependence of this fiber device becomes more intensive and spectral spacing of the individual beams that can exhibit distinct propagations becomes small as the length of the MM fiber is increased [27–29]. Consequently in the 10 nm band spectral components that their incoherent addition contributes to the formation of the bright central spot are increased. The facet and the far-field intensity profiles of the 10 cm long MM fiber are shown in Figs. 5 (a)-(d) and (e)-(h), respectively. We also notice that, the fringe visibility of the far-field profile of the beam coming from the 10 cm long MM fiber is smaller compared to that of the beam coming from the 2 cm long MM fiber. This may be caused by the coupling of the power from LP_{0n} modes to the LP_{mn} modes ($m>1$) due to the geometrical imperfections of the MM fiber.

According to the calculations shown in Fig. 3 and our previous demonstrations [20,28], nondiffracting propagation distance can be increased by increasing the core diameter of the MM fiber. Then a 2 cm long MM fiber with a core diameter of 105 μm is used in our experiment. A white light Bessel-like beam with nondiffracting propagation distance of nearly 3 mm is obtained. The intensity profiles at the 105 μm MM fiber facet are shown in Figs. 6 (a)-(d) for the white, red, green, and blue light, respectively. Apparently, since more high order LP_{0n} modes are excited, the facet profiles exhibit patterns with more surrounding rings. And their far-field intensity profiles also have more ring patterns. Note that, since the physics of the Bessel beam generation of the fiber device is completely different from that of the axicon, the far-field intensity profile of the white light Bessel beam has almost the same visibility as that of the individual beams, as shown in Figs. 6 (e)-(h). The propagation characteristics of the white, red, green, and blue beams are shown in Figs. 6 (i)-(l), respectively. For the 2 cm long 105 μm MM fiber, the individual beams of the spectral components have bright central spot only at some certain positions and the addition of these beams gives the Bessel-like propagation characteristics of the white light.

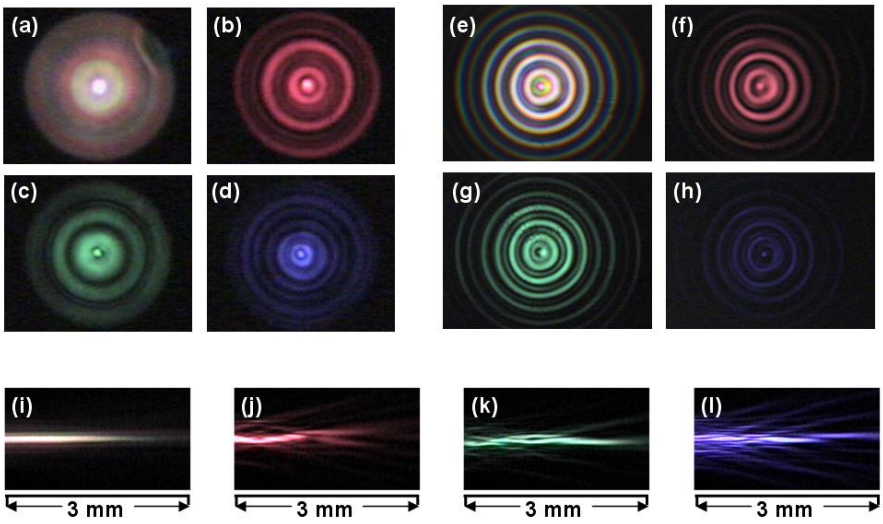

Fig. 6. Facet (a-d) and far-field (e-h) intensity profiles and the propagation characteristics (i-l) of the white Bessel beam and the red (630 nm), green (550 nm), and blue (480 nm) individual beams when a 2 cm long 105 μm multimode fiber is used.

In order to investigate the possibility of using a very large core MM fiber, a 200 μm core diameter MM fiber is spliced to the 460-HP fiber. Although the bare fiber diameter of the AFS200/220Y is 220 μm, which is much larger than the 125 μm diameter of the 460-HP fiber, a good splicing of the two fibers can still be obtained by using a common Ericsson fusion splicer. The facet and the far-field intensity profiles are shown in Figs. 7 (a)-(d) and (e)-(h), respectively. All of them show the pronouncing features of the Bessel beam. Note that, in order to record the whole far-field intensity profiles of the beam coming from the 200 μm

#143457 - $15.00 USD Received 2 Mar 2011; revised 27 Apr 2011; accepted 15 May 2011; published 26 May 2011

fiber, the CCD camera is placed at a position with a distance of 1 cm to the MM fiber facet. The propagation profiles of the white, red, green, and blue beams are shown in Figs. 7 (i)-(l). Because the 200 μm fiber cannot be fixed in the V-groove and is slant with a small angle, the propagation profile is a little bit oblique. The white light Bessel-like beam experiences a very small spreading in the propagation distance of 4 mm. Most interestingly, the propagation profiles of the individual beams exhibit several separated on-axis bright segments. This is because the constructive interference of the $LP_{0,n}$ modes on the axis occurs sparsely when over 60 modes are excited. According to the experiments of the 50 μm fiber, we can increase the length of these bright segments by increasing the MM fiber length and individual Bessel-like

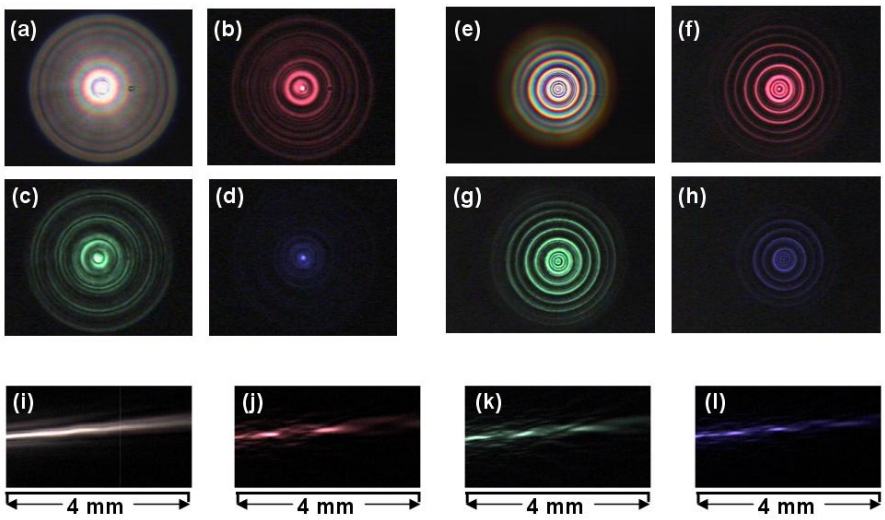

Fig. 7. Facet (a-d) and far-field (e-h) intensity profiles and the propagation characteristics (i-l) of the white Bessel beam and the red (630 nm), green (550 nm), and blue (480 nm) individual beams when a 2 cm long 200 μm multimode fiber is used.

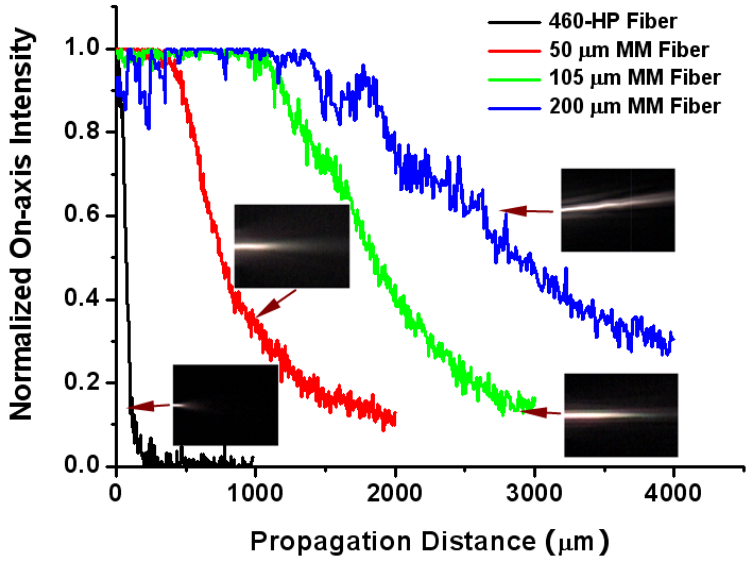

Fig. 8. Normalized on-axis intensity of the beams coming from the 460-HP single mode fiber (black) and the 2 cm long 50 μm (red), 105 μm (green), and 200 μm (blue) MM fibers.

#143457 - $15.00 USD Received 2 Mar 2011; revised 27 Apr 2011; accepted 15 May 2011; published 26 May 2011

beams like these shown in Fig. 5 can even be obtained if the MM fiber is long enough. Therefore, as has been stated in [20], the propagation profiles of the individual beams can be controlled by using MM fibers with different lengths.

The propagation characteristics of the white light beam directly coming from the single mode fiber 460-HP is also measured as a reference and shown in the inset of Fig. 8. The beam is subject to the diffraction and spreads out very quickly within 100 μm propagation distance. The on-axis intensities of the beams coming from the 460-HP single mode fiber and the 2 cm long 50 μm, 105 μm, and 200 μm MM fibers are plotted in Fig. 8. Because the propagation of the beam is completely determined by the facet field, which is strongly dependent on the MM fiber length [20,28], it is not appropriate to give a formula to describe the accurate relation between the distance of nondiffracting propagation and the core diameter based on the present experimental results. Nevertheless, it is rational to conclude that the distance of nondiffracting propagation increases with increasing core diameter of the MM fiber. Therefore, the distance of nondiffracting propagation can be approximately designed by choosing the core diameter of the MM fiber.

4. Analysis and Discussion

When a MM optical fiber is spliced onto a single mode optical fiber, the fundamental mode of the single mode fiber is decomposed to multiple $LP_{0,n}$ modes of the MM fiber. The larger the core size of the MM fiber, the more high order $LP_{0,n}$ modes are excited. Because high order $LP_{0,n}$ mode is closely resemble to the Bessel beams, nondiffracting beam can be generated from the large-core MM fiber [20,28]. Likewise, as the single mode white light is coupled to the MM fiber, white light propagation invariant beam can be generated from the MM fiber. Therefore, the physics of the fiber device is different from that of the axicon, which generates Bessel beam through the interference of the plane waves propagating on a conic surface. White light Bessel beams generated by the fiber device also have different characteristics and properties from the Bessel beams generated by axicons. Moreover, because the single mode fiber has a core diameter of about 3 μm, the fiber device offers an inherent highly spatial coherence, which is the prerequisite for the generation of white light Bessel-like beam with long distance of invariant propagation and many surrounding rings.

Our experiments demonstrate that white light propagation invariant beam can be generated from this fiber device even when a temporally incoherent broadband light source is used. The distance of nondiffracting propagation of the white light Bessel beam and the propagation characteristics of the individual beams of the spectral components can be easily and widely manipulated through the parameters including the length of the MM fiber segment and the core diameter of the MM fiber segment.

It needs to make clear that the distance of nondiffracting propagation of a Bessel beam is usually shorter than the Rayleigh range of a Gaussian beam with the same beam size [10]. For this fiber device, Bessel-like beam is created from the addition of high order $LP_{0,n}$ modes propagating in free space and high order $LP_{0,n}$ modes always experience a larger diffraction than low order $LP_{0,n}$ modes, especially the fundamental mode ($LP_{0,1}$ mode), so the distance of nondiffracting propagation of the Bessel-like beam is much shorter than the Rayleigh range of the $LP_{0,1}$ mode, which is equal to $\pi\omega_0^2/\lambda$ (here, ω_0 is the mode field radius of the $LP_{0,1}$ mode). It is also generally known that nondiffracting propagation of Bessel beam is achieved by sacrificing most of its power in the surrounding rings, i.e. only a small fraction of power is confined in the central bright spot. Seen from the far-field intensity profiles of the Bessel-like beams, the central spot contains a small amount of power due to its extremely small size. As the core size of the MM fiber increases, the power percentage of the central spot reduces accordingly. However, as a gain, the distance of nondiffracting propagation increases with the increasing core size.

It is worthwhile to note that the single mode signal delivery fiber is compatible with the microstructure fiber that has been frequently used for supercontinuum generation. It is feasible to build a compact, monolithic, and alignment-free all-fiber system to generate strong white light Bessel-like beam.

#143457 - $15.00 USD Received 2 Mar 2011; revised 27 Apr 2011; accepted 15 May 2011; published 26 May 2011

5. Conclusion

We demonstrated that white light Bessel-like beam can be generated from a miniature fiber device consisting of a single mode white light delivery fiber and a MM optical fiber. The simple and compact all-fiber device not only can create well-controllable white light propagation invariant beam, but also can offer the freedom of controlling the propagation of the individual Bessel beams of the spectral components. This fiber device may enable the multiple-functional workstation such as the integration of the optical traps and the spectroscopic sensors.

Acknowledgments

This work is supported by the National Sciences Foundation through grant No. 0725479 and the state of Arizona TRIF Photonics Initiative.

#143457 - $15.00 USD Received 2 Mar 2011; revised 27 Apr 2011; accepted 15 May 2011; published 26 May 2011